Investigation of the Dependence of the Rate of Cyclohexene Alkoxycarbonylation with Cyclohexanol and CO on the *p*-Toluenesulfonic Acid Monohydrate Concentration and Temperature

N. T. Sevostyanova[a],* and S. A. Batashev[a]

[a] Tula State Lev Tolstoy Pedagogical University, Tula, 300026 Russia
**e-mail: sevostyanova.nt@gmail.com*

Abstract—The effects of the *p*-toluenesulfonic acid monohydrate (TsOH·H$_2$O) concentration on the alkoxycarbonylation of cyclohexene over a Pd(PPh$_3$)$_2$Cl$_2$–PPh$_3$–TsOH·H$_2$O catalytic system were quantified at 363–383 K. Within this temperature range, the correlation between the cyclohexyl cyclohexanecarboxylate production rate and the TsOH·H$_2$O concentration was found to be similar to an S-shaped curve. Based on these data, as well as previous findings with regard to the effects of water and TsOH·H$_2$O concentrations on the cyclohexene methoxycarbonylation rate, the hydride mechanism for the alkoxycarbonylation process was updated by adding relevant ligand exchange reactions between *ballast* palladium complexes, specifically reactions that produce a palladium aqua complex. The accordingly-modified kinetic equation for cyclohexene alkoxycarbonylation with cyclohexanol and CO was found to be consistent with the experimental data. Effective constants were evaluated for the modified kinetic equation over the studied temperature range. A number of relevant parameters—namely, the effective activation energy and the changes in enthalpy, entropy, and Gibbs free energy during the ligand exchange between the complexes Pd(PPh$_3$)$_2$(C$_6$H$_{11}$OH)$_2$ and Pd(PPh$_3$)$_2$(H$_2$O)$_2$—were further evaluated in light of the activated complex theory. This reaction was found to be nearly equilibrium at 373 K.

Keywords: alkoxycarbonylation, cyclohexene, cyclohexanol, carbon monoxide, effective activation energy, ligand exchange

The development of the unsaturated compounds alkoxycarbonylation with alcohols and CO has advanced considerably in recent decades. For this process, a wide variety of alkenes have been used, from ethylene [1, 2] to heavy alkenes, including those branched along multiple bonds [3, 4] and polymers with C=C bonds [5]. Not only petrochemicals but also unsaturated vegetable compounds have been used as substrates [6–8]. Alkoxycarbonylation can be carried out in the presence of Pd, Rh, Ru, Ir, Ir, Pt, Os, Co, Ni, Mo, W, Cr, and Sn catalysts [9]. In recent decades, research has mostly focused on homogeneous palladium–phosphine catalytic systems, which are commonly assumed to be the most catalytically active [1–8, 10–12]. Industrial production of methyl methacrylate over a catalyst of this sort has

been implemented using Lucite's Alpha process [8, 12]. Furthermore, some recent studies have successfully used Co- and Ru-based catalysts. For example, a commercially valuable reaction such as the propoxycarbonylation of ethylene was catalyzed by homogeneous Co$_2$(CO)$_8$-based systems [13], and the methoxycarbonylation of diisobutylene (2,3,4-trimethylpent-1-ene) was carried out over supported cobalt catalysts [14]. Studies have also been published on the methoxycarbonylation of cyclohexene over homogeneous ruthenium catalysts [15, 16] and the methoxycarbonylation of ethylene over heterogeneous ruthenium catalysts [17]. Among the most promising alkoxycarbonylation approaches, special attention should be drawn to the so-called isomerizing alkoxycarbonylation of alkenes with internal multiple

bonds over palladium catalysts with some diphosphines [5, 8, 10, 11]. This process consists of two successive steps: migration of the C=C bond to the terminal position; and alkoxycarbonylation that preferentially produces linear esters. Yang et al [18] recently investigated an isomerizing alkoxycarbonylation process as part of the industrially relevant selective synthesis of adipinates from 1,3-butadiene.

Isomerizing alkoxycarbonylation can also occur *via* the dehydration of secondary alcohols catalyzed by strong protonic acids such as *p*-toluenesulfonic acid monohydrate (TsOH·H_2O) and the resulting *in situ* formation of internal alkenes [19]. In particular, when a linear secondary alcohol (e.g., 2-hexanol, 2-heptanol, or 2-nonanol) was used, its dehydration and the alkoxycarbonylation of the resultant internal alkene were arranged in one reactor to preferentially produce a linear carboxylic ester (2-hexyl heptanoate, 2-heptyl octanoate, and 2-nonyl decanoate, respectively). When cyclohexanol was used as a model alcohol in the dehydration combined in one reactor with the subsequent cyclohexene alkoxycarbonylation, the yield of cyclohexyl cyclohexanecarboxylate (CHCHC) reached up to 86% over 4–6 h. In this process, the strong protonic acids played a key role: under their effect, the yield of cyclohexene amounted to 20–34% within the initial 25–30 min [19, 20]. However, the cyclohexene alkoxycarbonylation rates were insufficient [19–22]. In alkoxycarbonylation over homogeneous palladium catalysts, relatively inactive *ballast* species are known to form and negatively affect the formation rate of target products [3, 23–25]. In-depth kinetic studies on the effects of various reactants on the reaction rate are able to shed light on these patterns and enable researchers to assess the relative stability of the various ballast complexes in the alkoxycarbonylation system [24]. We have previously investigated the effects of different reactants, Pd(PPh$_3$)$_2$Cl$_2$ (as a catalytic precursor), and PPh$_3$ (as a promoter) on the rate of cyclohexene alkoxycarbonylation with cyclohexanol and CO (reaction (1)) [23, 25]. We believe that to gain deeper insight into the mechanism of this reaction, the kinetics of the TsOH·H_2O concentration effect on the reaction also need to be investigated in detail. It is worth noting that cyclohexane carboxylic esters are of significant practical interest as intermediates in pharmaceutical synthesis [9], and cyclohexene is a convenient model substrate with an internal C=C bond because its alkoxycarbonylation produces a single ester. Cyclohexanol is an available

large-tonnage secondary alcohol. In contrast to methanol, an alcohol most commonly used in alkoxycarbonylation [1–8, 12, 14], other alcohols—including secondary alcohols—have been underexplored as contributors to alkoxycarbonylation.

$$\text{(1)}$$
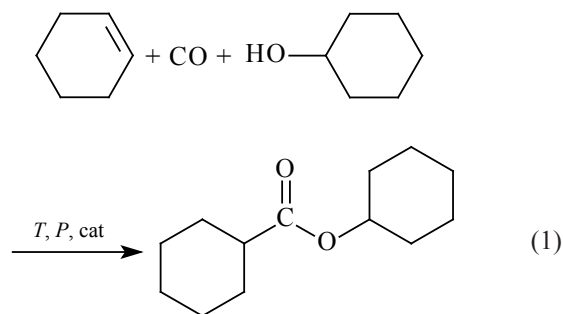
EXPERIMENTAL

The details of the reactor, as well as the methods employed for the kinetic study of alkoxycarbonylation and for the gas chromatography of the reaction mixture samples using *o*-xylene as an internal standard, are described in Supplementary Information. The correlation between the cyclohexene alkoxycarbonylation rate and the TsOH·H_2O concentration was investigated in a toluene medium at P_{CO} = 2.1 MPa with the following initial concentrations being used in all experiments (mol/L): c_0 (C$_6$H$_{10}$) = 0.100; c_0 (C$_6$H$_{11}$OH) = 0.400; c_0 (Pd(PPh$_3$)$_2$Cl$_2$) = 2.0×10^{-3}; and c_0 (PPh$_3$) = 8.0×10^{-3}. The reaction mixture samples were tested on a *Tsvet 162* chromatograph equipped with a flame ionization detector and 3000×3 mm glass columns. The separation was carried out using a *Chromaton* N-AW-DMCS packing (0.125 to 0.160 mm particles) with a 5% XE-60 stationary phase at an argon carrier gas flow rate of 30 mL/min and an injector temperature of 250°C. The temperature was programmed to ramp up from 65 to 205°C at a rate of 12°C/min. Chromatographic peaks were identified by comparing the retention times of the components in the test samples with those in commercial cyclohexene and cyclohexanol samples and in a synthesized CHCHC sample. The CHCHC synthesis procedure is described in [19], and its NMR and IR spectra are provided in that article's Supplementary Information. The concentrations both of the reactants and the products were measured with an accuracy of ±3%. The confidence intervals (CIs) of the kinetic parameters are provided in the body of that article. The test data on the steel reactor resistance
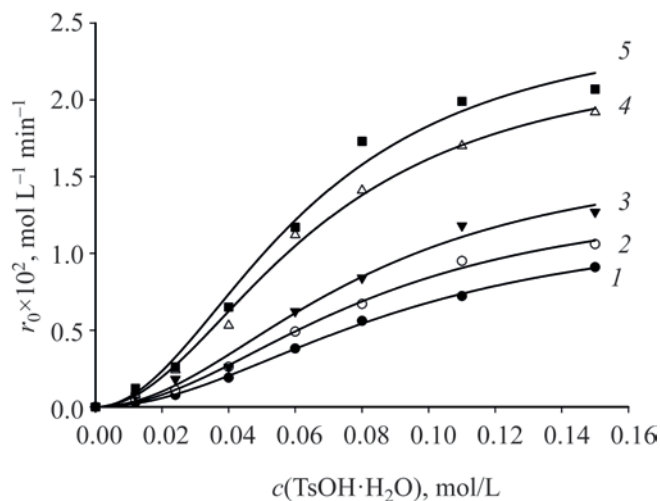
Fig. 1. Rate of cyclohexene alkoxycarbonylation with cyclohexanol and CO as a function of TsOH·H$_2$O concentration at various temperatures (K): (*1*) 363; (*2*) 368; (*3*) 373; (*4*) 378; and (*5*) 383. Reaction conditions: P_{CO} = 2.1 MPa; initial concentrations (mol/L): c_0 (C$_6$H$_{10}$) = 0.100; c_0 (C$_6$H$_{11}$OH) = 0.400; c_0(Pd(PPh$_3$)$_2$Cl$_2$) = 2.0×10^{-3}; c_0 (PPh$_3$)=8.0×10^{-3}.

in a TsOH·H$_2$O environment and the evaluation of the potential diffusion effects on the reaction rate are provided in the Supplementary Information of the present article.

RESULTS AND DISCUSSION

In order to investigate the effects of TsOH·H$_2$O concentration and process temperature on the rate of cyclohexene alkoxycarbonylation with cyclohexanol and CO, five series of experiments were carried out at 363–383 K, with the TsOH·H$_2$O concentration varying from 0 to 0.150 mol/L in each series. Like the kinetic curves previously plotted for an identical reaction [23], the CHCHC accumulation curves were roughly S-shaped, with a short induction period of 5–10 min. The initial alkoxycarbonylation rates were determined using the initial sections of the kinetic curves following the induction period. These initial sections, which included 4–6 data points (in accordance with the number of reaction mixture samples), were approximated by straight lines (with a correlation coefficient of at least 0.985). The line slopes were taken as the initial reaction rates. Figure 1 illustrates the initial reaction rates (indicated by the dots on the curves) at varying TsOH·H$_2$O concentrations and temperatures.
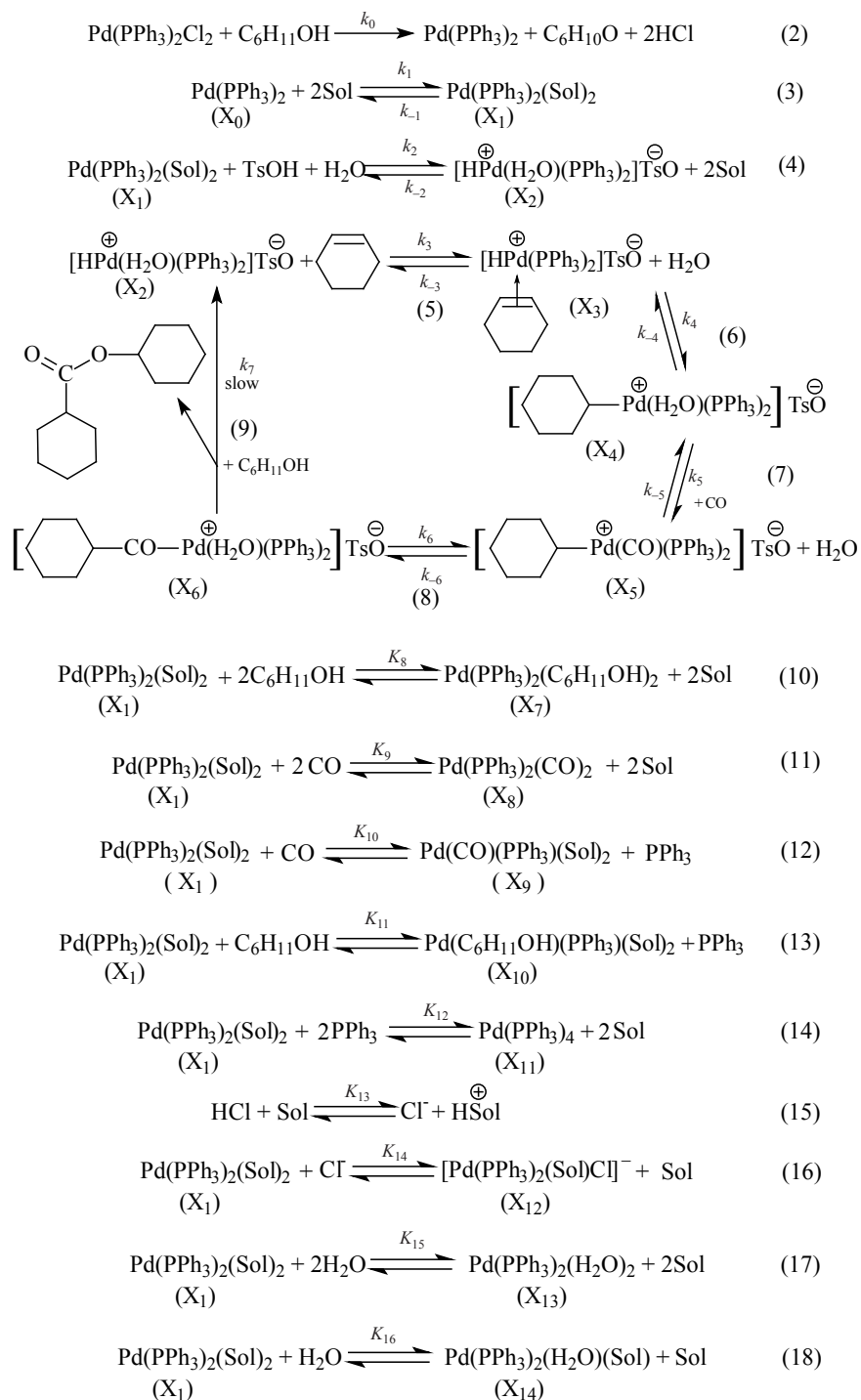
In recent decades, it has been commonly assumed that the alkoxycarbonylation of unsaturated compounds over palladium–phosphine catalytic systems with strong protonic acids occurs by a hydride mechanism [5–8]. In our previous studies on the effects of different reactants, Pd(PPh$_3$)$_2$Cl$_2$, and PPh$_3$ on the rate of cyclohexene alkoxycarbonylation with cyclohexanol and CO, we suggested that this hydride mechanism additionally involves ligand exchange reactions that produce inactive (*ballast*) Pd complexes [23, 24]. In particular, the following reaction involving one TsOH molecule was formulated for the formation of a hydride complex (which is the key intermediate in the hydride mechanism for alkoxycarbonylation):

$$Pd(PPh_3)_2(Sol)_2 + TsOH$$
$$\leftrightarrow [HPd^+(Sol)(PPh_3)_2] + TsO^- + Sol.$$
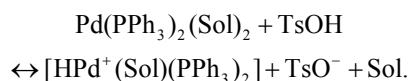
In more recent research we used a Pd(OAc)$_2$–PPh$_3$–TsOH·H$_2$O catalytic system with TsOH·H$_2$O concentrations up to 6.4×10^{-2} M, and the cyclohexene methoxycarbonylation rate was found to vary as a parabolic function of the TsOH·H$_2$O concentration and as an extremal function of the concentration of the added water [25]. This extremal dependence reflected an accelerating effect of minor amounts of water on methoxycarbonylation and a slowdown of this reaction at higher water concentrations in the reaction mixture. These patterns were explained in the context of an updated version of the hydride mechanism, according to which the formation of the hydride palladium complex involves one TsOH molecule and one H$_2$O molecule. The experimental data were found to be consistent with a new kinetic equation derived for cyclohexene methoxycarbonylation [25]. In the present study, for cyclohexene alkoxycarbonylation with cyclohexanol and CO, we made a similar update to the hydride mechanism previously proposed in [23, 24] by adding ligand exchange reactions (17) and (18). These reactions produce ballast Pd complexes under the effect of water (Scheme 1, reactions (10)–(18), where Sol denotes the toluene solvent molecules).

Taking into account this modification as well as the negligible contribution of reactions (12) and (13) to the total balance of reactions in the system under study (as found in [24]), the previously proposed kinetic equation

Scheme 1. Hydride mechanism for cyclohexene alkoxycarbonylation with cyclohexanol and CO [reactions (2)–(9)], with additional formation of ballast Pd complexes [reactions (10)–(18)].

$$Pd(PPh_3)_2Cl_2 + C_6H_{11}OH \xrightarrow{k_0} Pd(PPh_3)_2 + C_6H_{10}O + 2HCl \qquad (2)$$

$$\underset{(X_0)}{Pd(PPh_3)_2} + 2Sol \underset{k_{-1}}{\overset{k_1}{\rightleftharpoons}} \underset{(X_1)}{Pd(PPh_3)_2(Sol)_2} \qquad (3)$$

$$\underset{(X_1)}{Pd(PPh_3)_2(Sol)_2} + TsOH + H_2O \underset{k_{-2}}{\overset{k_2}{\rightleftharpoons}} \underset{(X_2)}{[\overset{\oplus}{H}Pd(H_2O)(PPh_3)_2]\overset{\ominus}{T}sO} + 2Sol \qquad (4)$$

$$\underset{(X_1)}{Pd(PPh_3)_2(Sol)_2} + 2C_6H_{11}OH \xrightarrow{K_8} \underset{(X_7)}{Pd(PPh_3)_2(C_6H_{11}OH)_2} + 2Sol \qquad (10)$$

$$\underset{(X_1)}{Pd(PPh_3)_2(Sol)_2} + 2CO \xrightarrow{K_9} \underset{(X_8)}{Pd(PPh_3)_2(CO)_2} + 2Sol \qquad (11)$$

$$\underset{(X_1)}{Pd(PPh_3)_2(Sol)_2} + CO \xrightarrow{K_{10}} \underset{(X_9)}{Pd(CO)(PPh_3)(Sol)_2} + PPh_3 \qquad (12)$$

$$\underset{(X_1)}{Pd(PPh_3)_2(Sol)_2} + C_6H_{11}OH \xrightarrow{K_{11}} \underset{(X_{10})}{Pd(C_6H_{11}OH)(PPh_3)(Sol)_2} + PPh_3 \qquad (13)$$

$$\underset{(X_1)}{Pd(PPh_3)_2(Sol)_2} + 2PPh_3 \xrightarrow{K_{12}} \underset{(X_{11})}{Pd(PPh_3)_4} + 2Sol \qquad (14)$$

$$HCl + Sol \xrightarrow{K_{13}} Cl^- + H\overset{\oplus}{S}ol \qquad (15)$$

$$\underset{(X_1)}{Pd(PPh_3)_2(Sol)_2} + Cl^- \xrightarrow{K_{14}} \underset{(X_{12})}{[Pd(PPh_3)_2(Sol)Cl]^-} + Sol \qquad (16)$$

$$\underset{(X_1)}{Pd(PPh_3)_2(Sol)_2} + 2H_2O \xrightarrow{K_{15}} \underset{(X_{13})}{Pd(PPh_3)_2(H_2O)_2} + 2Sol \qquad (17)$$

$$\underset{(X_1)}{Pd(PPh_3)_2(Sol)_2} + H_2O \xrightarrow{K_{16}} \underset{(X_{14})}{Pd(PPh_3)_2(H_2O)(Sol)} + Sol \qquad (18)$$

Table 1. Effective constants in Eq. (21)

Temperature, K	363	368	373	378	383
(k_{eff}/A), L mol^{-1} min^{-1}	0.145±0.022	0.165±0.031	0.164±0.051	0.372±0.066	0.314±0.049
$(j/A)\times10^{-2}$, L^2/mol^2	1.22±0.10	1.42±0.11	1.42±0.18	2.03±0.18	1.93±0.14
(l/A), L/mol	−1.0±3.2	−5.0±5.0	−8.9±9.2	−7.8±8.0	−13.0±14.2

for cyclohexene alkoxycarbonylation with cyclohexanol and CO (Eq. (10) in [24]) takes the following form:

$$r_0 = \frac{kc_{Pd}c_0(C_6H_{10})c_0(C_6H_{11}OH)[CO]c_0(TsOH)c_0(H_2O)}{1 + dc_0^2(C_6H_{11}OH) + e[CO]^2 + hc_0^2(PPh_3) + nc_{Pd} + jc_0^2(H_2O) + lc_0(H_2O)},$$

(19)

where r_0 is the initial alkoxycarbonylation rate;

$$k = \frac{k_7 K_1 K_2 K_3 K_4 K_5 K_6}{1 + K_1}, \ d = \frac{K_1 K_8}{1 + K_1}, \ e = \frac{K_1 K_9}{1 + K_1}, \ h = \frac{K_1 K_{12}}{1 + K_1},$$

$$n = \frac{2 K_1 K_{13} K_{14}}{[H^+Sol](1 + K_1)}, \ j = \frac{K_1 K_{15}}{1 + K_1}, \ l = \frac{K_1 K_{16}}{1 + K_1},$$

c_{Pd} is the total concentration of all Pd forms: $c_{Pd} = [X_0] + [X_1] + ... + [X_8] + [X_{11}] + ... + [X_{14}]$, matching the initial concentration of Pd(PPh$_3$)$_2$Cl$_2$.

Given that TsOH·H$_2$O is the only water source in the system, Eq. (19) transforms into:

$$r_0 = \frac{kc_{Pd}c_0(C_6H_{10})c_0(C_6H_{11}OH)[CO]c_0^2(TsOH\cdot H_2O)}{1 + dc_0^2(C_6H_{11}OH) + e[CO]^2 + hc_0^2(PPh_3) + nc_{Pd} + jc_0^2(TsOH\cdot H_2O) + lc_0(TsOH\cdot H_2O)}.$$

(20)

Under the single-factor experimental conditions with respect to TsOH·H$_2$O, Eq. (20) can be simplified:

$$r_0 = \frac{k_{eff}c_0^2(TsOH\cdot H_2O)}{A + jc_0^2(TsOH\cdot H_2O) + lc_0(TsOH\cdot H_2O)} \ \text{or}$$

$$r_0 = \frac{\dfrac{k_{eff}}{A}c_0^2(TsOH\cdot H_2O)}{1 + \dfrac{j}{A}c_0^2(TsOH\cdot H_2O) + \dfrac{l}{A}c_0(TsOH\cdot H_2O)}, \quad (21)$$

where $k_{eff} = kc_{Pd}c_0(C_6H_{10})c_0(C_6H_{11}OH)[CO]$; and $A = 1 + dc_0^2(C_6H_{11}OH) + e[CO]^2 + hc_0^2(PPh_3) + nc_{Pd}$.

Table 1 presents the parameters of Eq. (21) derived using the Sigma Plot 11.0 package.

The data of Table 1 clearly show that (l/A) is statistically negligible. In all probability, Eq. (21) does not optimally describe the experimental data obtained in the study, especially given that no strong correlations were observed in the variations of (k_{eff}/A) and (j/A) with a temperature increase. With (l/A) being statistically negligible, Eq. (21) was converted to Eq. (22), the parameters of which are presented in Table 2:

$$r_0 = \frac{\dfrac{k_{eff}}{A}c_0^2(TsOH\cdot H_2O)}{1 + \dfrac{j}{A}c_0^2(TsOH\cdot H_2O)}.$$

(22)

Using the parameters of Table 2, the r_0 variation as a function of c_0 (TsOH·H$_2$O) is graphically illustrated in Fig. 1. At all the tested temperatures, the experimental data (indicated by the dots) were well fitted by Eq. (22). Most probably, reaction (18) does not make a major contribution to the overall reaction balance in this system.

Using the values of the effective constants (k_{eff}/A) and (j/A) indicated in Table 2, the effective constants (j/k_{eff})

Table 2. Effective constants in Eq. (22)

Temperature, K	363	368	373	378	383
(k_{eff}/A), L mol^{-1} min^{-1}	0.151±0.010	0.210±0.012	0.266±0.030	0.532±0.040	0.643±0.078
$(j/A)\times10^{-2}$, L^2/mol^2	1.23±0.10	1.49±0.13	1.58±0.27	2.29±0.24	2.51±0.42
(j/k_{eff}), m^3 s mol^{-1}	48.9	42.6	35.6	25.8	23.4
$(j'/k'_{eff})\times10^{-12}$, mol^2 s Pa m^{-6}	8.324	7.252	6.060	4.392	3.983

were derived. For these constants, the following equation holds true:

$$\frac{j}{k_{eff}} = \frac{K_1 K_{15}}{(1+K_1)kc_{Pd}c_0(C_6H_{10})c_0(C_6H_{11}OH)[CO]}$$

$$= \frac{K_1 K_{15} H_{CO}(1+K_1)}{(1+K_1)k_7 K_1 K_2 K_3 K_4 K_5 K_6 c_{Pd}c_0(C_6H_{10})c_0(C_6H_{11}OH)P_{CO}}$$

$$= \frac{K_{15} H_{CO}}{k_7 K_2 K_3 K_4 K_5 K_6 c_{Pd}c_0(C_6H_{10})c_0(C_6H_{11}OH)P_{CO}}, \quad (23)$$

where H_{CO} is Henry's equilibrium constant for the CO–toluene system.

With a new parameter being further introduced:

$$\frac{j'}{k'_{eff}} = \frac{j}{k_{eff}} c_{Pd}c_0(C_6H_{10})c_0(C_6H_{11}OH)P_{CO}, \quad (24)$$
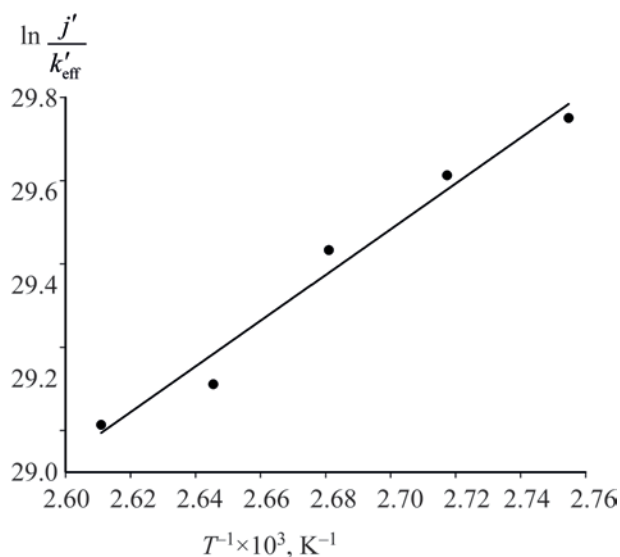
Fig. 2. Arrhenius function for effective constant (j'/k'_{eff}).

we arrived at the following equation:

$$\frac{j'}{k'_{eff}} = \frac{K_{15} H_{CO}}{k_7 K_2 K_3 K_4 K_5 K_6}. \quad (25)$$

The values of (j'/k'_{eff}) are also presented in Table 2. Special attention should be drawn to a significant rise in (k_{eff}/A) and (j/A) between 373 and 378 K. This rise can likely be attributed to overall errors (both upward and downward) in the calculation of individual (k_{eff}/A) and (j/A) constants within the tested range of 363–383 K. In fact, these parameters represent combinations of a variety of equilibrium constants applicable to different steps of the tested reaction. For a less sophisticated parameter such as (j'/k'_{eff}), we see a smaller difference between the values for 373 and 378 K.

The (j'/k'_{eff}) behavior fitted the Arrhenius function with a correlation coefficient of 0.986 (Eq. (26); Fig. 2):

$$\frac{j'}{k'_{eff}} = 10^{6.366} \exp\left(\frac{46\pm1 \text{ kJ/mol}}{RT}\right), \frac{\text{mol}^2 \text{ s Pa}}{\text{m}^6}. \quad (26)$$

In [24], an Arrhenius correlation was obtained for the effective constant $(d/k_{eff\,4})$:

$$\frac{d}{k_{eff\,4}} = 10^{-7.30} \exp\left(\frac{54\pm4 \text{ kJ/mol}}{RT}\right), \frac{\text{m}^6 \text{ s}^2}{\text{mol}^2}. \quad (27)$$

According to the findings of [24], the constant $(d/k_{eff\,4})$ is described fairly well by the equation:

$$\frac{d}{k_{eff\,4}} = \frac{K_1 K_8}{(1+K_1)kc_{Pd}c_0(C_6H_{10})[CO]c_0(TsOH\cdot H_2O)}$$

$$= \frac{K_1 K_8 H_{CO}(1+K_1)}{(1+K_1)k_7 K_1 K_2 K_3 K_4 K_5 K_6 c_{Pd}c_0(C_6H_{10})c_0(TsOH\cdot H_2O)P_{CO}}$$

$$= \frac{K_8 H_{CO}}{k_7 K_2 K_3 K_4 K_5 K_6 c_{Pd}c_0(C_6H_{10})c_0(TsOH\cdot H_2O)P_{CO}}. \quad (28)$$

Within the framework of Eq. (27), the following holds true at 373 K:

$$\frac{d}{k_{\text{eff }4}} = 1.83 \frac{\text{m}^6 \text{ s}^2}{\text{mol}^2}.$$

A new parameter was further introduced:

$$\frac{d'}{k'_{\text{eff }4}} = \frac{d}{k_{\text{eff }4}} c_{\text{Pd}} c_0 (\text{C}_6\text{H}_{10}) P_{\text{CO}} c_0 (\text{TsOH} \cdot \text{H}_2\text{O})$$

$$= \frac{K_8 H_{\text{CO}}}{k_7 K_2 K_3 K_4 K_5 K_6}. \tag{29}$$

Using the initial experimental conditions imposed in the previous study regarding the effect of the cyclohexanol concentration on the cyclohexene alkoxycarbonylation rate [24], this constant was calculated as follows:

$$\frac{d'}{k'_{\text{eff }4}} = 1.83 \cdot 0.002 \cdot 0.1 \cdot 21 \cdot 101325 \cdot 0.024 \times 10^9$$

$$= 1.87 \times 10^{10} \frac{\text{mol Pa s}^2}{\text{m}^3}. \tag{30}$$

The following was derived from Eq. (25) in combination with Eq. (29):

$$\frac{j'}{k'_{\text{eff}}} : \frac{d'}{k'_{\text{eff }4}} = \frac{K_{15}}{K_8},$$

and therefore: $\ln (j'/k'_{\text{eff}}) - \ln (d'/k'_{\text{eff }4}) = \ln K_{15} - \ln K_8$.

Based on the effective activation energies found above, we arrived at:

$$\ln \frac{j'}{k'_{\text{eff}}} - \ln \frac{d'}{k'_{\text{eff }4}} = \frac{\Delta S_{15} - \Delta S_8}{R} - \frac{\Delta H_{15} - \Delta H_8}{RT} + \ln H_{\text{CO}} - \ln H_{\text{CO}},$$

and, consequently:

$$\ln \frac{j'}{k'_{\text{eff}}} - \ln \frac{d'}{k'_{\text{eff }4}} = \frac{\Delta S_{15} - \Delta S_8}{R} - \frac{\Delta H_{15} - \Delta H_8}{RT}. \tag{31}$$

The differential between the two effective activation energies equals to:

$$E\left(\frac{j'}{k'_{\text{eff}}}\right) - E\left(\frac{d'}{k'_{\text{eff }4}}\right) = \Delta H_{15} - \Delta H_8,$$

which resulted in:

$$\Delta H_{15} - \Delta H_8 = -46 - (-54) = 8 \text{ kJ/mol}. \tag{32}$$

The following was reasonably derived from Eq. (31):

$$\Delta S_{15} - \Delta S_8 = R \left(\ln \frac{j'}{k'_{\text{eff}}} - \ln \frac{j'}{k'_{\text{eff}}} + \frac{\Delta H_{15} - \Delta H_8}{RT} \right). \tag{33}$$
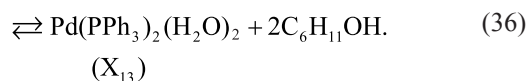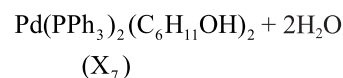
Using Eq. (26), (j'/k'_{eff}) was evaluated at 373 K:

$$\frac{j'}{k'_{\text{eff}}} = 6.43 \times 10^{12} \frac{\text{mol}^2 \text{ Pa s}}{\text{m}^6}. \tag{34}$$

Based on Eq. (33), and using the effective constants evaluated above in (30) and (34), we obtained:

$$\Delta S_{15} - \Delta S_8 = 8.314 \ln \left(\frac{6.43 \times 10^{12}}{1.87 \times 10^{10}} + \frac{8000}{8.314 \cdot 373} \right) = 70 \frac{\text{J}}{\text{mol} \cdot \text{K}}. \tag{35}$$

The values of $\Delta H = \Delta H_{15} - \Delta H_8$ and $\Delta S = \Delta S_{15} - \Delta S_8$ reflect the enthalpy and entropy changes during the ligand exchange between the two complexes:

$$\text{Pd(PPh}_3)_2 (\text{C}_6\text{H}_{11}\text{OH})_2 + 2\text{H}_2\text{O}$$
$$(\text{X}_7)$$
$$\rightleftarrows \text{Pd(PPh}_3)_2 (\text{H}_2\text{O})_2 + 2\text{C}_6\text{H}_{11}\text{OH}. \tag{36}$$
$$(\text{X}_{13})$$

At 373 K, the Gibbs free energy change for this reaction amounted to:

$$\Delta G = 8 - 373 \cdot 70 \times 10^{-3} = -18 \text{ kJ/mol}.$$

Thus, the ΔH value shows the weakly endothermic nature of reaction (36). We see that the binding energy between one cyclohexanol molecule and the Pd site in the complex X_7 was about 4 kJ/mol higher than the binding energy of the water molecule in the complex X_{13}. Therefore, under the conditions of reaction (1), X_7 was

more stable and less reactive than X_{13}. This is consistent with the common assumption of more pronounced donor–acceptor properties of alcohols than those of water. The positive ΔS (see the above calculations) can likely be explained by the fact that two H_2O molecules (small-sized) were bound and two cyclohexanol molecules (medium-sized) were released. On the other hand, the ΔG value indicates that, under the conditions of cyclohexene alkoxycarbonylation with cyclohexanol in the presence of TsOH·H_2O, reaction (36) is near equilibrium.

CONCLUSIONS

Within the temperature range of 363–383 K, the dependence between the rate of cyclohexene alkoxy-carbonylation with cyclohexanol and CO and the concentration of TsOH·H_2O was found to be similar to an S-shaped curve. Based on the kinetic data obtained in this study, as well as our previous findings with regard to the effects of water and TsOH·H_2O concentrations on the cyclohexene methoxycarbonylation rate, the hydride mechanism for the alkoxycarbonylation process was updated by adding relevant ligand exchange reactions between *ballast* palladium complexes, specifically reactions that produce a palladium aqua complex. The accordingly-modified kinetic equation for cyclohexene alkoxycarbonylation with cyclohexanol and CO was found to be consistent with the experimental data. Effective constants were evaluated for the modified kinetic equation over the studied temperature range. The new data on the effects of the TsOH·H_2O concentration, in combination with the previous findings on the cyclohexanol concentration effects on the cyclohexene alkoxycarbonylation rate between 368 and 388 K, enabled us to further evaluate, in light of the activated complex theory, a number of relevant parameters: the effective activation energy and the changes in enthalpy, entropy, and Gibbs free energy during the ligand exchange between the complexes $Pd(PPh_3)_2(C_6H_{11}OH)_2$ and $Pd(PPh_3)_2(H_2O)_2$. This reaction was found to be near equilibrium at 373 K.

AUTHOR INFORMATION

N.T. Sevostyanova, ORCID: http://orcid.org/0000-0002-3499-2226

S.A. Batashev, ORCID: http://orcid.org/0000-0001-7537-7740

CONFLICT OF INTEREST

The authors declare no conflict of interest requiring disclosure in this article.

SUPPLEMENTARY INFORMATION

The online version contains supplementary material available at https://doi.org/10.1134/S0965544124040042.

REFERENCES

1. Kalck, Ph. and Urrutigoïty, M., *Inorg. Chim. Acta*, 2015, vol. 431, pp. 110–121.
   https://doi.org/10.1016/j.ica.2015.02.007

2. García-Suárez, E.J., Khokarale, S.G., van Buu, O.N., Fehrmann, R., and Riisager, A., *Green Chem.*, 2014, vol. 16, no. 1, pp. 161–166.
   https://doi.org/10.1039/C3GC41380B

3. Nifant'ev, I.E., Sevostyanova, N.T., Batashev, S.A., Vinogradov, A.A., Vinogradov, A.A., Churakov, A.V., and Ivchenko, P.V., *Appl. Catal. A: Gen.*, 2019, vol. 581, pp. 123–132.
   https://doi.org/10.1016/j.apcata.2019.05.030

4. Nobbs, J.D., Low, C.H., Stubbs, L.P., Wang, C., Drent, E., and van Meurs, M., *Organometallics*, 2017, vol. 36, no. 2, pp. 391–398.
   https://doi.org/10.1021/acs.organomet.6b00813

5. Liu, Y., Dong, K., Beller, M., and Mecking, S., *ACS Catal.*, 2018, vol. 8, no. 10, pp. 9232–9237.
   https://doi.org/10.1021/acscatal.8b03117

6. Biermann, U., Bornscheuer, U.T., Feussner, I., Meier, M.A.R., and Metzger, J.O., A*ng. Chem. Int. Ed.*, 2021, vol. 60, no. 37, pp. 20144–20165.
   https://doi.org/10.1002/anie.202100778

7. Nomura, K. and Awang, N.W.B., *ACS Sust. Chem. Eng.*, 2021, vol. 9, no. 16, pp. 5486–5505.
   https://doi.org/10.1021/acssuschemeng.1c00493

8. Sevostyanova, N.T. and Batashev, S.A., *Catal. Ind.*, 2023, vol. 15, no. 4, pp. 333–349.
   https://doi.org/10.1134/S2070050423040104

9. Lapidus, A.L. and Pirozhkov, S.D., *Russ. Chem. Rev.*, 1989, vol. 58, no. 2, pp. 117–137.
   https://doi.org/10.1070/RC1989v058n02ABEH003430

10. Neubert, P., Steffen, M., and Behr, A., *J. Mol. Catal. A: Chem.*, 2015, vol. 407, pp. 122–127.
https://doi.org/10.1016/j.molcata.2015.06.019

11. Goldbach, V., Krumova, M., and Mecking, S., *ACS Catal.,* 2018, vol. 8, no. 6, pp. 5515–5525.
https://doi.org/10.1021/acscatal.8b00981

12. Mahboub, M.J.D., Dubois, J.-L., Cavani, F., Rostamizadeh, M., and Patience, G.S., *Chem. Soc. Rev.*, 2018, vol. 47, no. 20, pp. 7703–7738.
https://doi.org/10.1039/c8cs00117k

13. Gorbunov, D.N., Nenasheva, M.V., and Kardashev, S.V. *Russ. J. Appl. Chem.*, 2019, vol. 92, no. 8, pp. 1069–1076.
https://doi.org/10.1134/S1070427219080032

14. Song, H., Lei, S., Jin, F., and Liu, H., *Mol. Catal.*, 2022, vol. 527, Art. 112408.
https://doi.org/10.1016/j.mcat.2022.112408

15. Wu, L., Liu, Q., Jackstell, R., and Beller, M., *Org. Chem. Front.*, 2015, vol. 2, no. 7, pp. 771–774.
https://doi.org/10.1039/C5QO00071H

16. Sevostyanova, N.T. and Batashev, S.A., *Russ. J. Phys. Chem. B*, 2018, vol. 12, no. 3, pp. 593–594.
https://doi.org/10.1134/S1990793118030296

17. An, J., Wang, Y., Lu, J., Zhang, J., Zhang, Z., Xu, S., Liu, X., Zhang, T., Gocyla, M., Heggen, M., Dunin-Borkowski, R.E., Fornasiero, P., and Wang, F., *J. Am. Chem. Soc.*, 2018, vol. 140, no. 11, pp. 4172–4181.
https://doi.org/10.1021/jacs.8b01742

18. Yang, J., Liu, J., Ge, Y., Huang, W., Ferretti, F., Neumann, H., Jiao, H., Franke, R., Jackstell, R., and Beller, M., *Angew. Chem. Int. Ed.*, 2021, vol. 60, no. 17, pp. 9527–9533.
https://doi.org/10.1002/anie.202015329

19. Sevostyanova, N.T., Batashev, S.A., Rodionova, A.S., and Kozlenko, D.K., *Tetrahedron*, 2023, vol. 146, Art. 133653.
https://doi.org/10.1016/j.tet.2023.133653

20. Sevostyanova, N.T., Batashev, S.A., and Rodionova, A.S., *Russ. Chem. Bull.*, 2023, vol. 72, no. 8, pp. 1936–1939.
https://doi.org/10.1007/s11172-023-3980-1

21. Eliseev, O.I., Bondarenko, T.N., Stepin, N.N., and Lapidus, A.L., *Mendeleev Commun.*, 2006, vol. 16, no. 2, pp. 107–109.
https://doi.org/10.1070/MC2006v016n02ABEH002232

22. Dong, K., Sang, R., Liu, J., Razzaq, R., Franke, R., Jackstell, R., and Beller, M., *Angew. Chem. Int. Ed.*, 2017, vol. 56, no. 22, pp. 6203–6207.
https://doi.org/10.1002/anie.201701950

23. Aver'yanov, V.A., Sevost'yanova, N.T., Batashev, S.A., and Nesolenaya, S.V., *Petrol. Chem.*, 2006, vol. 46, no. 6, pp. 405–414.
https://doi.org/10.1134/S0965544106060053

24. Aver'yanov, V.A., Sevost'yanova, N.T., and Batashev, S.A., *Petrol. Chem.*, 2008, vol. 48, no. 4, pp. 287–295.
https://doi.org/10.1134/S0965544108040063

25. Averyanov, V.A., Sevostyanova, N.T., Batashev, S.A., Vorobiev, A.A., and Rodionova, A.S., *Russ. J. Phys. Chem. B*, 2014, vol. 8, no. 2, pp. 140–147.
https://doi.org/10.1134/S1990793114020031